Biochimica et Biophysica Acta 1850 (2015) 299–306

Contents lists available at ScienceDirect

Biochimica et Biophysica Acta

journal homepage: www.elsevier.com/locate/bbagen

# Antibacterial effect of silver nanoparticles and the modeling of bacterial growth kinetics using a modified Gompertz model

Tanaya Chatterjee [a,*], Barun K. Chatterjee [b], Dipanwita Majumdar [b], Pinak Chakrabarti [a,c]

[a] Department of Biochemistry, Bose Institute, P-1/12 CIT Scheme VIIM, Kolkata 700054, India
[b] Department of Physics, Bose Institute, 93/1 A.P.C. Road, Kolkata 700009, India
[c] Bioinformatics Centre, Bose Institute, P-1/12 CIT Scheme VIIM, Kolkata 700054, India

ARTICLE INFO

*Article history:*
Received 28 June 2014
Received in revised form 17 October 2014
Accepted 21 October 2014
Available online 27 October 2014

*Keywords:*
Silver nanoparticle
Antibacterial activity
Growth kinetics
Death rate
Gompertz model
Logistic model

ABSTRACT

*Background:* An alternative to conventional antibiotics is needed to fight against emerging multiple drug resistant pathogenic bacteria. In this endeavor, the effect of silver nanoparticle (Ag-NP) has been studied quantitatively on two common pathogenic bacteria *Escherichia coli* and *Staphylococcus aureus*, and the growth curves were modeled.
*Methods:* The effect of Ag-NP on bacterial growth kinetics was studied by measuring the optical density, and was fitted by non-linear regression using the Logistic and modified Gompertz models. Scanning Electron Microscopy and fluorescence microscopy were used to study the morphological changes of the bacterial cells. Generation of reactive oxygen species for Ag-NP treated cells were measured by fluorescence emission spectra.
*Results:* The modified Gompertz model, incorporating cell death, fits the observed data better than the Logistic model. With increasing concentration of Ag-NP, the growth kinetics of both bacteria shows a decline in growth rate with simultaneous enhancement of death rate constants. The duration of the lag phase was found to increase with Ag-NP concentration. SEM showed morphological changes, while fluorescence microscopy using DAPI showed compaction of DNA for Ag-NP-treated bacterial cells.
*Conclusions: E. coli* was found to be more susceptible to Ag-NP as compared to *S. aureus*. The modified Gompertz model, using a death term, was found to be useful in explaining the non-monotonic nature of the growth curve.
*General significance:* The modified Gompertz model derived here is of general nature and can be used to study any microbial growth kinetics under the influence of antimicrobial agents.


## 1. Introduction

Study of microbial growth curve is a fundamental aspect of predictive microbiology and is indispensable in diverse fields of biotechnology, genetics, ecology, etc. [1,2]. Predictive microbiology is a combination of statistical, mathematical and microbiological principles to quantify the behavior of a particular microorganism [3]. The most common pattern for bacterial growth is a lag phase before replication, followed by exponential growth to reach maximum population density, which eventually goes to "death phase" [4]. Modeling of bacterial growth kinetics enables one to describe the behavior of a particular microorganism under different environmental conditions and hence appropriate models are needed to extract parameters from such growth curves [5]. Microbial growth curves are characterized by a sigmoidal shape and various mathematical models are proposed to fit the curves [6,7]. Among various models, two popular mathematical models reported in literature are the Logistic model and Gompertz model [8,9]. However, the inability of the Logistic model to generate a sigmoidal curve on a semi-logarithmic plot led to the development of a modified Logistic model [10]. The Gompertz model is one of the most extensively used mathematical model which was originally introduced to describe the mortality rate of humans [11]. Later on Gibson et al. modified the Gompertz model to better fit the bacterial growth [12]. The modified Gompertz model is extensively used in predictive microbiology software programs such as Pathogen Modeling Program introduced by United States Department of Agriculture (http://www.arserrc.gov/mfs/).

The last couple of decades have seen emergence of multiple-drug resistant bacterial pathogens endangering human health [13,14]. Among various pathogenic bacteria, some strains of *Escherichia coli* and *Staphylococcus aureus* show resistance against β-lactum containing common antibiotics, such as penicillin, ampicillin, and methicillin [15,16]. This has led to flurry of activities looking for appropriate alternatives to treat various debilitating diseases; nanoparticles have been identified as potential candidate in the field of clinical medicine [17,18]. Silver

*Abbreviations:* Ag-NP, silver nanoparticle; $H_2$DCF-DA, dichlorofluorescein diacetate; DAPI, 4′,6-diamidino-2-phenylindole; PI, propidium iodide; FCC, face-centered cubic; ROS, reactive oxygen species; OD, optical density

* Corresponding author. Tel.: +91 33 2569 3253; fax: +91 33 2355 3886.
*E-mail addresses:* tanaya@jcbose.ac.in, tanaya_chatterjee@yahoo.com (T. Chatterjee).

http://dx.doi.org/10.1016/j.bbagen.2014.10.022
0304-4165/

nanoparticles (Ag-NP) possess excellent biocidal properties against a wide variety of microorganisms, and have attracted wide attention [19,20]. Considering the importance of toxicity of engineered nanoparticles on physiological system, Ag-NP has been found to show higher toxicity to microorganisms compared to human cells [21]. Recent literature reports interaction of Ag-NP with human immunodeficiency virus type 1 via preferential binding to the gp120 glycoprotein knobs, thereby inhibiting the virus from binding to host cells [22]. In the present paper, the effect of Ag-NP on the growth kinetics of *E. coli* and *S. aureus*, representing Gram negative and Gram positive bacteria, respectively, has been made using the modified Logistic and the Gompertz models. The incorporation of a "death term" in the latter model provides a quantitative approach to gain insight into the growth kinetics of two commonly used bacterial strains.

The antimicrobial action of Ag-NP occurs due to penetration of nanoparticle inside bacterial cell membrane, thereby suppressing respiratory enzymes [23]. Moreover, they interfere with DNA components inside the bacterial cells resulting in the prevention of its replication and transcription [24,25]. A series of experiments have been conducted for the understanding of the mode of inactivation of the bacterial growth by Ag-NP. Fluorescence based assays using fluorochromes are widely used to detect the state of individual cells, such as membrane integrity, and intracellular enzymatic activity [26–28]. In the present study we have used DAPI, a cell-permeable dsDNA specific stain to confirm the morphology of nucleoids of both *E. coli* and *S. aureus* after treatment with Ag-NP. Moreover, the surface morphology of the Ag-NP-treated *E. coli* cells was compared with the untreated cells by scanning electron microscope (SEM).

Flow cytometry is an extensively used method for determining cell viability. In the present paper cell viability for both bacteria on treatment with Ag-NP was assessed by staining with membrane impermeant dye, propidium iodide (PI). The PI has its unique feature of penetrating cell membrane of dead cells, but viable cells are excluded [29]. There are reports on the formation of highly reactive oxygen species (ROS), such as $OH^-$, $H_2O_2$ and $O_2^{2-}$, which are responsible for the antibacterial activity of Ag-NP, causing cell death [30]. In the present study the inhibitory as well as lethal effects of Ag-NP on bacterial cells, were assessed spectrofluorimetrically using $H_2$DCF-DA.

## 2. Theory

### 2.1. Modeling bacterial growth kinetics incorporating death

The kinetics of the growth of bacterial populations (viz. *E. coli* and *S. aureus*) has been modeled by the ubiquitous Logistic and the Gompertz models [8,9]. The data were fitted using non-linear regression to both these models. Bacterial growth by the Logistic model can be given as

$$\frac{dN}{dt} = rN\left(1-\frac{N}{N_x}\right) \tag{1}$$

where $N$ is the number of bacterial cells present, $r$ is an effective growth rate constant for Logistic model and $N_x$ is the asymptotic value of $N$. In the absence of competition and death, the growth rate of a bacterium would be exponential, and saturation indicates the presence of these constraints. The effect of Ag-NP would be to enhance death, and this perturbation can be introduced in this model as a first order term (the death term) in $N$ indicating an uncorrelated and random process. It can be demonstrated here that the introduction of the death term does not change the functional form of the Logistic equation, since,

$$\frac{dN}{dt} = rN\left(1-\frac{N}{N_x}\right) - Nd = r'N\left(1-\frac{N}{N_x'}\right) \tag{2}$$

where $d$ is the death rate constant gives back a similar monotonic equation with changed parameters. Here

$$r' = r - d \tag{3}$$

and

$$N_x' = N_x(r-d)/r \tag{4}$$

and for $r' > 0$ the curve displays monotonic growth from $N_0$ to a maximum value of $N_x'$, while for $r' < 0$ it is a monotonic decline from $N_0$ to zero. Death is reflected in how $r'$ varies with the introduction of silver nanoparticles. The solution of Eq. (2) is

$$N = \frac{N_0 N_x'}{N_0 + (N_x - N_0')e^{-r't}} \tag{5}$$

which is identical in form to the solution when the death rate is not included.

The delay after which the bacterial growth curve rises sharply can be quantitatively defined as the time where the tangent to the curve at the maximum slope intersects the line parallel to time axis through $N_0$ [31]. This delay time, which is an indicator of the duration of the lag phase, is given for the Logistic model as

$$t_{lag} = \frac{1}{r'}\ln\left(\frac{N_x'}{N_0} - 1\right) - \frac{2}{r'}\left(1 - \frac{2N_0}{N_x'}\right). \tag{6}$$

The bacterial growth rates can also be modeled using the Gompertz model as

$$\frac{dN}{dt} = rbNe^{-rt}. \tag{7}$$

Here, death ($d$) can be introduced in this model as

$$\frac{dN}{dt} = rbNe^{-rt} - Nd \tag{8}$$

The solution of this equation is

$$N = a\exp\left(-be^{-rt} - td\right) \tag{9}$$

which is, however, non-monotonic. This has a maximum at

$$t = \frac{1}{r}\ln\left(\frac{rb}{d}\right) \tag{10}$$

and

$$N_{\max} = N_x\left(\frac{erb}{d}\right)^{-d/r}. \tag{11}$$

Here the initial slope is $N_0(-d + rb)$ which is positive for $d < rb$. The delay time can be quantitatively given as

$$t_{lag} = -\frac{1}{r}\ln\left(c + \frac{1}{2b} + \sqrt{\frac{1}{4b^2} + \frac{c}{b}}\right) - \frac{2}{r\left(1+\sqrt{1+4bc}\right)}\left\{1 - e^{\left[-b - \frac{d}{r}\ln\left(c + \frac{1}{2b} + \sqrt{\frac{1}{4b^2}+\frac{c}{b}}\right) + \frac{d}{r} + \frac{1}{2} + \sqrt{\frac{1}{4}+\frac{d}{r}}\right]}\right\} \tag{12}$$

where $c = d/br$. In the absence of death, this delay is simply $\frac{1}{r}\left[\ln(b/e) + e^{(-b+1)}\right]$.

It is thus evident that the Gompertz model, though simple, is amenable to the incorporation of death in explaining the non-monotonic nature of bacterial growth curves. One should also note that this feature

affects the growth curve in the realm of the growth phase when the mortality phase [9] (which takes place at much longer time-scales, even in the absence of Ag-NP) has not yet set in.

## 3. Materials and methods

### 3.1. Materials

Silver nitrate ($AgNO_3$) and sodium borohydride ($NaBH_4$) were purchased from SRL (Mumbai, India). DAPI and $H_2$DCF-DA were purchased from Sigma. These reagents were used without further purification. The bacteria *E. coli* K12 and *S. aureus* MTCC 3160 used in this study were obtained from the Institute of Microbial Technology (Chandigarh, India).

### 3.2. Synthesis and characterization of Ag-NP

Ag-NP was synthesized as reported previously using $AgNO_3$ as metal salt precursor [32].

The concentration of atomic silver ([Ag]) has been considered here, while the corresponding concentration of silver nanoparticle ([Ag-NP]) would be

$$[\text{Ag-NP}] = \frac{6M[\text{Ag}]}{\pi\rho d^3 N_A} = 4.76[\text{Ag}] \times 10^{-6} \quad (13)$$

where $\rho$ is the density of silver (10.5 g $cm^{-3}$ for the FCC structure), $d$ is the mean diameter of the nanoparticle (19 nm), $M$ is the atomic weight of silver (108) and $N_A$ is the Avogadro number. This however assumes that the nanoparticles are homogeneous solid spheres, without voids or irregularities. Since only the concentration of silver (irrespective of its aggregation) can be provided unambiguously, while that of Ag-NP depends on the size and the assumed density of the silver in the nanoparticles, the molar concentration of silver will be used all through the text.

The synthesized Ag-NP was characterized by UV–visible spectroscopy and Transmission Electron Microscopy (TEM). Spectroscopic studies were carried out using Lambda-25, Perkin Elmer spectrophotometer and TEM measurements were performed using JEOL 2010 microscope with LaB6 filament operated at 200 kV.

### 3.3. Effect of Ag-NP on bacterial growth kinetics

Bacterial cells were cultured in 5 mL of Luria Bertani (LB) media at 37 °C for overnight. Cells from the overnight culture (2% inoculums) were then transferred to 50 mL of LB along with varying concentrations of Ag-NP and incubated at 37 °C with continuous agitation. The Ag-NP concentration in culture media varied from 10 μM to 50 μM, which was directly calculated from the final molar concentration of silver. A flask without Ag-NP was kept as control to track the normal growth of the bacterial cells. To monitor growth trends, samples were withdrawn aseptically at each 30 min interval and OD of the cells was measured at 595 nm on a Shimadzu UV Spectrophotometer UV-1800. The reference used was the same LB without bacteria.

### 3.4. Colony counting assay for bacterial susceptibility to Ag-NP

For colony counting assay bacterial suspensions from overnight culture (both *E. coli* and *S. aureus*) were inoculated in LB (concentration of $10^5$ CFU/mL was used) and supplemented with different concentrations of Ag-NP. The cultures at specified time interval were withdrawn aseptically, and cell suspensions were serially diluted with sterile Phosphate Buffer Saline (PBS, pH 7.2), and finally spread onto LB agar plates. Ag-NP-free LB plates cultured under the same condition were used as control. The plates were then incubated further at 37 °C for 24 h and the numbers of colonies were counted. The experiment was carried out in triplicates and the number of colonies for a particular set was averaged.

### 3.5. Assessment of cell viability after treatment with Ag-NP using flow cytometry

Cells from overnight culture of both *E. coli* and *S. aureus* were inoculated in fresh 5 mL of LB and shaken at 37 °C until the OD reached 0.4. Then cell cultures were incubated with requisite amount of Ag-NP for 1 h and the cells were harvested at 4000 rpm at 4 °C. Likewise, control cells without Ag-NP were also grown and harvested. The cell pellets were washed and finally resuspended in cold 1× PBS and incubated with RNase A (1 mg/mL stock) at room temperature for 1 h. Finally the cell suspensions were incubated with 5 μl of PI in dark for 10 min. The fluorescence was determined using a flow cytometer (FACSCalibur, BD Biosciences), equipped with a 488 nm argon laser light source using CellQuest software.

### 3.6. Detection of reactive oxygen species (ROS)

The detection of ROS generation by Ag-NP was carried out by staining cells with $H_2$DCF-DA [30]. A stock solution of 1 mg/mL was prepared in molecular grade DMSO (Sigma) and stored at −20 °C. Cells were grown to about $10^5$ CFU/mL in LB medium and incubated with 10 μg/mL of $H_2$DCF-DA for 60 min. After centrifugation, cells were washed and resuspended in sterile PBS. $H_2$DCF-DA fluorescence was determined in a Hitachi F-3010 spectrofluorimeter with a scanning speed of 240 nm per min in 1 cm path length quartz cuvette having both excitation and emission slit widths of 2.5 nm. Fluorescence emission spectra were recorded from 500 to 600 nm with an excitation wavelength of 492 nm. The emission maxima were recorded at 523 nm. Samples were run in triplicate.

### 3.7. Study of bacterial cells by fluorescence microscopy and scanning electron microscope (SEM)

Both *E. coli* and *S. aureus* cells were grown in LB at 37 °C overnight. From the overnight culture 2% inoculums were added to 5 mL of LB and shaken at 37 °C until the O.D. was reached 0.5. Then Ag-NP of varying concentrations were added, and incubated at 37 °C for 1 h. The control was maintained under the same condition without Ag-NP. Cell pellet was harvested at 5000 rpm for 10 min at 4 °C and washed twice with ice-cold PBS. The pellet was then resuspended in PBS and fixed in 2.5% of glutaraldehyde for 30 min at room temperature. The cell pellet was again harvested at 5000 rpm for 10 min at 10 °C and washed with ice cold PBS. Staining with DAPI (final concentration 2.5 μg/mL) was carried out by gently shaking in the rocker for 30 min. Cells were then washed twice with ice-cold PBS, and resuspended in PBS. Samples were taken on glass slides overlaid with cover slips using Kaiser's glycerol gelatin mix (Merck, India). Each slide was then viewed by Zeiss Axiovert 200 M fluorescence microscope under 100× oil D.I.C. objectives. DNA was visualized under 405 nm DAPI filter.

SEM was used to observe the morphological changes of *E. coli* cells induced by Ag-NP. The nanoparticle treated cells ($10^5$ CFU/mL) were centrifuged at 5000 rpm for 10 min and washed with PBS followed by fixing with 2.5% glutaraldehyde. The fixed cells were again washed with PBS and dehydration was carried out using 25, 50, 75, 90 and 100% of ethanol. After drying of the fixed cells, gold coating was carried out and the treated samples were observed by SEM.

## 4. Results

### 4.1. Characterization of Ag-NP

For structural characterization of Ag-NP, UV–vis spectroscopy is one of the most commonly used techniques. Fig. S1 (Supporting Information)

shows the optical absorption spectrum of Ag-NP and the observed absorption maximum ($\lambda_{max}$) at 397 nm is due to the dipolar surface plasmon of individual spherical silver particles. TEM was used to determine the particle size and the size distribution of Ag-NP. Fig. S2 (Supporting Information) provides the low magnification TEM micrograph and the histogram of the measured size of many particles. The particle size distribution is fitted with Gaussian function and from the fitting the estimated average particle size and standard deviation were 19 nm and 5 nm, respectively.

### 4.2. Bacterial growth kinetics at various Ag-NP concentrations

Assuming that the OD at 595 nm reflects the number density of bacterial cells, its value was found to increase in a sigmoidal fashion in the absence of Ag-NP. For *E. coli* cells, the usual sigmoidal growth was observed at 0 μM concentration of Ag-NP, which at higher concentrations (10, 20 and 30 μM), changed to a non-monotonic nature, reaching a maximum value and then declining with time (Fig. 1a). Growth of *S. aureus* cells also showed a similar trend, with a sigmoidal curve in the absence of Ag-NP, changing to a similar non-monotonic form in the presence of 20, 30, 40 and 50 μM of nanoparticles (Fig. 1b).

The growth and the death rate constants for *E. coli* as obtained from the modified Gompertz model are shown in Fig. 2a. The growth rate constant ($r$) decreases with increasing concentration of Ag-NP and can be represented as

$$r = 0.065 + 0.081e^{-0.3[\text{Ag-NP}]}\ \text{h}^{-1} \quad (14)$$

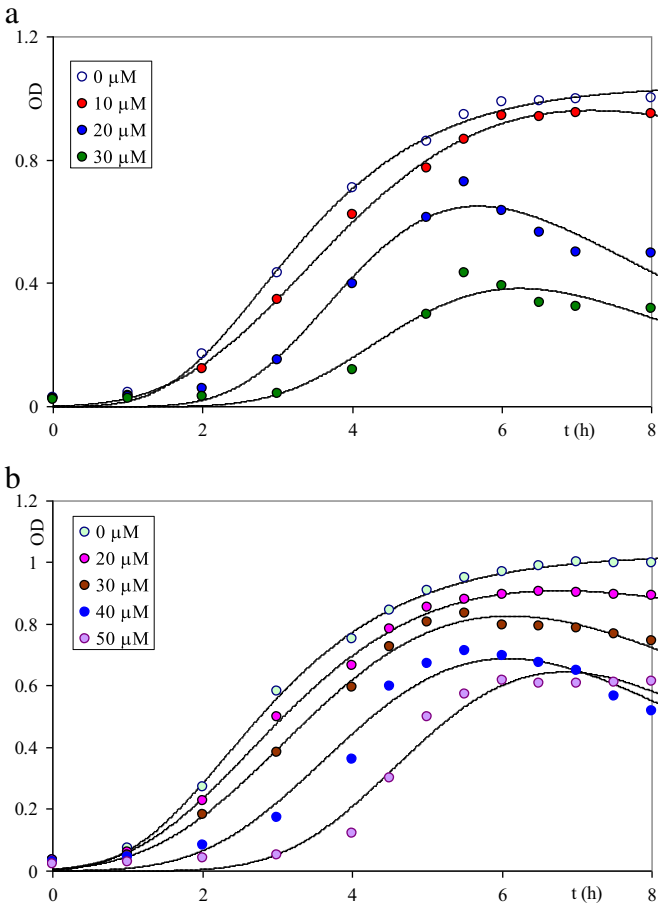


**Fig. 1.** Growth of (a) *E. coli* and (b) *S. aureus* cells with time. For both the bacteria the usual sigmoidal growth was observed at 0 μM Ag-NP, which at higher concentration changed to a non-monotonic form, reaching a maximum value and then declining.

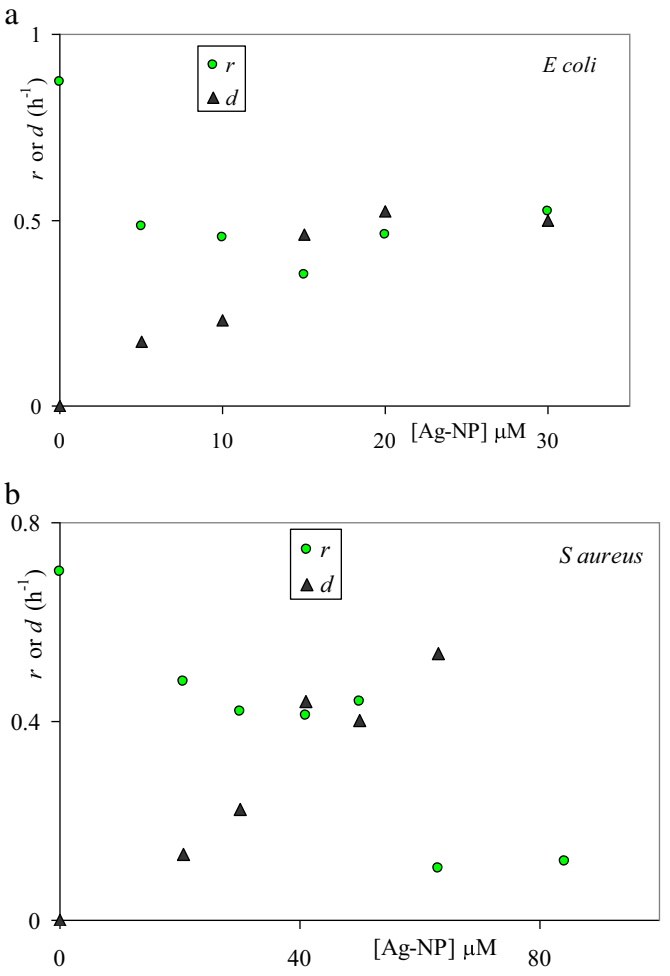


**Fig. 2.** Decrease in the growth rate constant ($r$) and increase of death rate constant ($d$) of (a) *E. coli* and (b) *S. aureus* with increase in the concentration of Ag-NP, as derived from the modified Gompertz model.

This probably implies that the *E. coli* cells adapt to the Ag-NP, and continue to grow at a reduced rate. Similarly, the death rate constant ($d$), for *E. coli* has been found to increase with increasing concentration of Ag-NP and

$$d = 0.0037[\text{Ag-NP}]\ \text{h}^{-1} \quad (15)$$

The growth rate constant for *S. aureus*, however, shows a steady decline (Fig. 2b) as evident from

$$r = 0.11 - 0.0012[\text{Ag-NP}]\ \text{h}^{-1} \quad (16)$$

which is probably indicative of lack of such an adaptation. The death rate constant ($d$) for *S. aureus* (Fig. 2b) varies as

$$d = 0.0015[\text{Ag-NP}]\text{h}^{-1} \quad (17)$$

The growth rate ($r$) and death rate ($d$) constants for both the bacteria are shown in Table 1. The maximum value of bacterial concentration is inferred from the maximum value of the OD. This, when plotted as a function of the Ag-NP concentration, can be interpolated to get the $IC_{50}$ values for both the bacteria. The $IC_{50}$ values for *E. coli* and *S. aureus* were found to be 28 μM and 61 μM, respectively (Table 1). The Logistic model displays a declining effective growth rate term ($r'$) with concentration of Ag-NP which could be due to a fall in the growth rate term ($r$) or an increase in the death rate term (Fig. 3).

**Table 1**
Growth parameters of *E. coli* and *S. aureus* and the effect of Ag-NP using the modified Gompertz model.

| Parameters | *E. coli*[a] | | *S. aureus*[b] | |
|---|---|---|---|---|
| | Without Ag-NP | With 30 μM [Ag-NP] | Without Ag-NP | With 30 μM [Ag-NP] |
| Growth rate constant ($r$) ($h^{-1}$) | 0.15 | 0.07 | 0.11 | 0.08 |
| Death rate constant ($d$) ($h^{-1}$) | – | 0.11 | – | 0.04 |
| Delay time (h) | 1.7 | 2.8 | 1.1 | 1.4 |
| Onset of decline (h) | – | 6.2 | – | 6.1 |
| Maximum growth rate (OD/h) | 0.34 | 0.16 | 0.27 | 0.24 |
| $IC_{50}$ (μM) | – | 28.1 | – | 61.0 |

[a] Based on Eqs. (14) and (15).
[b] Based on Eqs. (16) and (17).

### 4.3. Significance of delay time or prolonged lag phase for Ag-NP treated bacterial cells

The lag phase as described by Monod is one of the poorly understood growth phases, which is controlled by unknown regulatory mechanisms [33]. This is the phase which allows the bacterial cells to adapt to the new environmental condition. In order to ascertain the effect of Ag-NP on lag phases of both *E. coli* and *S. aureus*, the growth rates were measured at different concentrations of nanoparticle. This prolonged lag phase can be alternatively expressed in terms of "delay time" which is indicative of the time required for the bacteria to get to the reproductive stage. Fig. 4 shows a remarkable increase of delay time with increasing concentration of Ag-NP for both the bacteria. However, the increase in delay time of *E. coli* is more as compared to that of *S. aureus*. The increase in the delay time with the introduction of Ag-NP is indicative of a stress on the reproductive machinery for both bacteria [34].

### 4.4. Antimicrobial activity of Ag-NP using colony counting assay

Antibacterial assay was carried out on LB agar plates containing 30 μM and 40 μM of Ag-NP for *E. coli* and *S. aureus*, respectively. Approximately $10^5$ CFU/mL of cells were applied to the both the control (without Ag-NP) and Ag-NP treated plates. The number of bacterial colonies was reduced significantly in the presence of Ag-NP (Fig. S3).

### 4.5. Flow cytometric analysis of Ag-NP treated cells

Flow cytometry was used to study the cell viability of both *E. coli* and *S. aureus* after treatment with Ag-NP. The highly fluorescent and polar dye PI is commonly used for identifying dead cells in a population, because it only intercalates with the DNA of cells which lack membrane integrity [29]. This unique property of PI enables one to distinguish between non-viable cells having bright red fluorescence from non-fluorescent viable cells. In the present study, the density dot plot graphs Ag-NP treated *E. coli* and *S. aureus* cells showed increase in red fluorescence signal as compared to control cells, with an increase in cell populations (by ~10–14%) from the lower left to the lower right quadrant (Fig. S4), indicating cell death upon incubation with Ag-NP. This "cell death" may be attributed to the generation of ROS causing DNA damage after disruption of cell membrane (discussed below).

### 4.6. Detection of ROS in bacterial cells treated with Ag-NP

It has previously been reported that the antibacterial activity of Ag-NP is associated with the generation of reactive oxygen species (ROS), such as hydroxyl radical ($OH^-$) superoxide anion ($O^{2-}$) and singlet oxygen ($^1O_2$) [30]. Generation of ROS can induce damage of cell membrane, resulting in modification of DNA, lipids and cellular proteins leading to cell death [31]. To investigate the ROS generation in the bacterial cells after treatment with Ag-NP, a cell permeable dye $H_2$DCF-DA was used. After 1 h of incubation with $H_2$DCF-DA, significant increase in the fluorescence intensity was observed for Ag-NP treated bacterial cells, as compared to the untreated control cells (Fig. 5).

### 4.7. Analysis of cell morphology of E. coli and S. aureus after treatment with Ag-NP

Fluorescence microscopic analysis using DAPI stained *E. coli* and *S. aureus* cells showed shrinkage of DNA upon treatment with Ag-NP compared to untreated control cells (Fig. 6). This condensation of DNA may arise from the leakage of cytoplasmic contents of the damaged cells which is indicative of cell lysis caused due to increased cell membrane permeability. Likewise, the SEM image of the Ag-NP treated

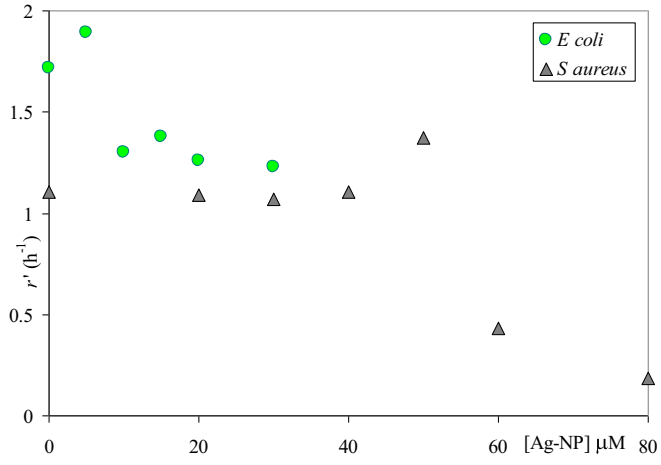


**Fig. 3.** The variation of growth rate constant from the Logistic model for *E. coli* and *S. aureus*.

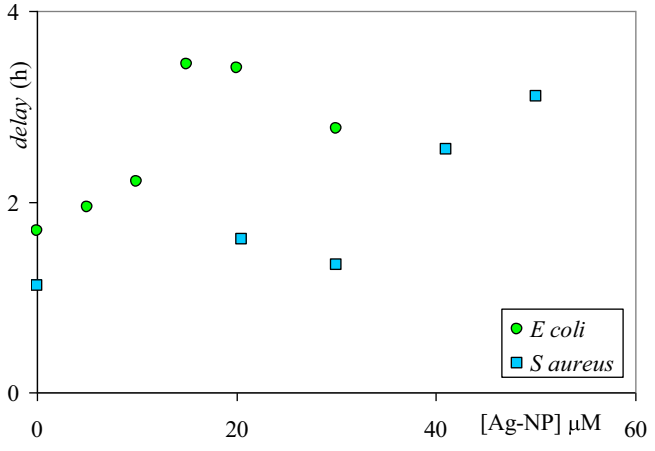


**Fig. 4.** Variation of delay time for *E. coli* and *S. aureus* as a function of the concentration of Ag-NP, as modeled by the modified Gompertz model.

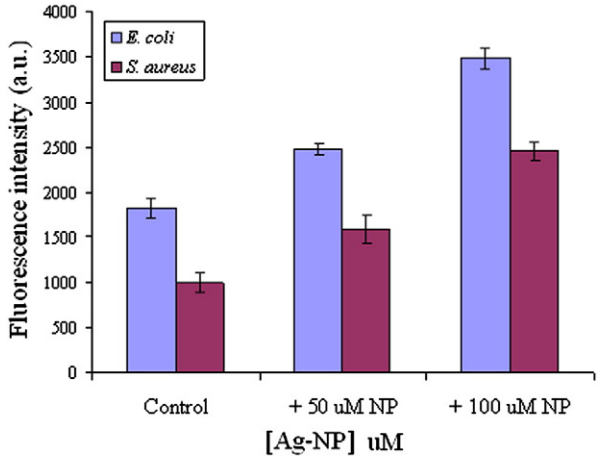


**Fig. 5.** Formation of ROS in *E. coli* and *S. aureus* cells on treatment with Ag-NP. Both control and Ag-NP treated bacterial cells were incubated with fluorescent dye $H_2$DCF-DA for 30 min.

*E. coli* cells (Fig. 7) showed rupture, abnormalities in cell shape and increase in length compared to untreated control cells.

## 5. Discussion

In this paper we have studied the bactericidal effect of Ag-NP on two representative bacteria, *E. coli* and *S. aureus*, and how their growth kinetics is affected by the presence of the nanoparticles. The bacterial growth was measured spectrophotometrically using OD. The use of OD for monitoring growth kinetics suffers from certain limitations, notably because it does not discriminate between live and dead cells. In spite of that, it still remains a widely used technique for its speed and simplicity [35]. As our intentions had been to model the effect of Ag-NP on the bacterial growth kinetics, and the incorporation of the death term, we have used OD as it is a more direct probe. However, it may be mentioned that the non-monotonic nature of the growth curves remains the same even when CFU/mL is used instead of OD (Fig. S5).

While simulating the growth, we demonstrated how the enhancement of death due to Ag-NP can be incorporated in the popular Logistic and Gompertz models. With increasing concentration of Ag-NP the growth kinetics of both bacteria show distinct decline in growth rate constants and increase of death rate constants (Fig. 2). For *E. coli* death ensued at about 10 μM, whereas in case of *S. aureus* cell death was evident around 20 μM of Ag-NP (Fig. 1).

Since lag phase has important implication for bacterial infection, the effect of Ag-NP on lag phases for both *E. coli* and *S. aureus* has been investigated. The lag phase, which comprises of the "adaptation phase" (lag1 phase) and the "first cell generation" (lag2 phase), increases in duration with increasing concentration of Ag-NP. The lag phase, and equivalently, the "delay time" have been found to increase for both the bacteria (Table 1). However, the existence of "prolonged lag phase" is found to be more for *E. coli* as compared to *S. aureus*, indicating higher susceptibility of the Gram negative *E. coli* than the Gram positive one.

Both the Logistic and the Gompertz models are simple enough to quantitatively describe the effect of Ag-NP on bacterial growth; however, the Logistic model does not have the mathematical features to explain the non-monotonic nature of the observed growth data. Additionally, the Gompertz model provides estimates for the death rate separately. Using the Logistic model no distinction can be made with respect to the cause of the decline in growth rate constant due to the Ag-NP, since from Eq. (3) the decline could be either due to the intrinsic decline of the growth rate constant, or due to the increase in the death rate, or both. The Logistic model has fewer parameters and hence the errors in the parameters by regression are expected to be lower, compared to Gompertz model. However, the Logistic model can only be used to fit the rising portion of the curve.

Though the mechanism of bactericidal actions of Ag-NP is still not well understood, several hypotheses have been proposed in the literature [36,37]. It is believed that the attachment of Ag-NP to the bacterial cell membrane causes the formation of "pits" on the bacterial cell walls, thereby allowing the nanoparticle to enter the periplasm of the bacterial

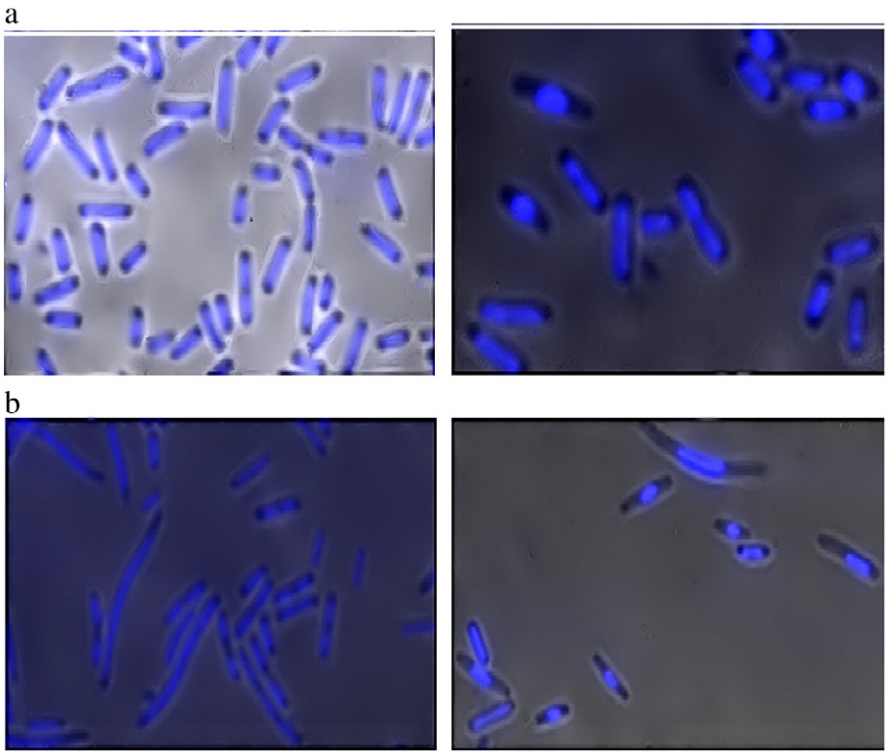


**Fig. 6.** DAPI stained (a) *E. coli* and (b) *S. aureus* cells (control in the left panel and 100 μM Ag-NP treated in the right panel) as viewed under Zeiss Axiovert 200 M fluorescence microscope.

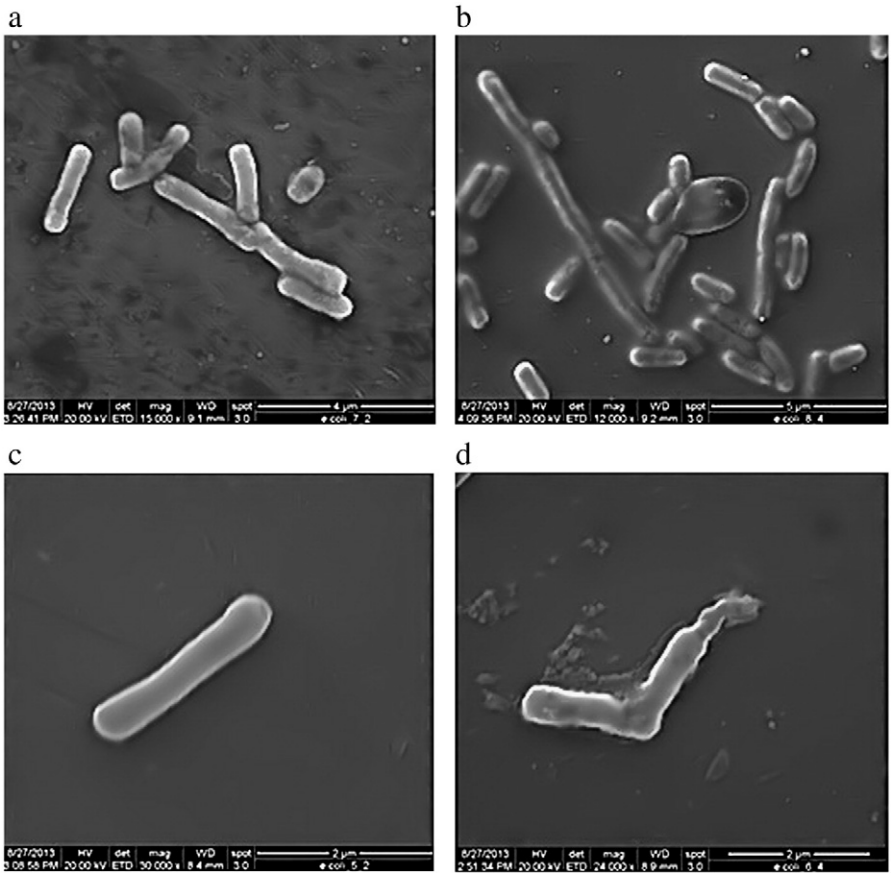


**Fig. 7.** SEM images showing the structure and morphology of (a) normal and (b) Ag-NP treated damaged *E. coli* cells. An isolated cell in the two cases is shown in (c) and (d), respectively.

cells [38]. As a result, subsequent alteration of DNA of Ag-NP treated bacterial cells leads to loss of replication ability of DNA and as a result the expression of proteins and enzymes essential for ATP production becomes inactivated [39,40]. In the present paper DAPI stained cells of both *E. coli* and *S. aureus* showed condensation of cellular DNA after treatment with Ag-NP, which probably occurs due to leakage of the cytoplasmic component of the damaged bacteria (Fig. 6). The presence of micromolar concentration of $Ag^+$ along with $Ag^0$ in Ag-NP is thought to be responsible for DNA damage [21]. Being a soft acid, $Ag^+$ has a tendency to react with soft bases containing phosphorous and sulfur, viz. $PR_3$, R-SH, R-S-R etc. and hence can preferentially interact with phosphorus-containing DNA and the sulfur-containing proteins of the cell [41].

In the present study *E. coli* cells have been found to be more susceptible upon treatment with Ag-NP, as compared to *S. aureus*, as evident from the $IC_{50}$ values. This difference of behavior may be attributed to the structural features of cell envelope of *E. coli* and *S. aureus*. Being Gram positive bacteria, the cell envelope of *S. aureus* consists of lipoteichoic acid along with thick peptidoglycan layer and cell membrane. The essential function of this thick peptidoglycan layer (30–100 nm thick) is to protect the cells against harmful reagents and hence the penetration of $Ag^+$ ions into the cytoplasm of *S. aureus* is prevented to some extent [37]. On the other hand, the cell envelop of *E. coli* consists of thin peptidoglycan layer along with the cell membrane and hence is more susceptible to Ag-NP [42].

The morphology of Ag-NP treated *E. coli* cells was studied using SEM. Though the *E. coli* cells of control group were typically rod-shaped, after treatment with Ag-NP, elongation and fragmentation of cells were observed. The formation of cell fragments was probably due to increased cell membrane permeability leading to the damage of cytoplasm [43].

The untreated and Ag-NP treated bacterial cells demonstrated noticeable difference in the viability in the present study as revealed by the antibacterial assay (Fig. S3). After treatment of Ag-NP, significant oxidative stress has been found to occur in both bacteria as evident from the increase in fluorescence intensity of $H_2$DCF-DA treated cells (Fig. 5). It may be anticipated that ROS (mainly $H_2O_2$) generation is facilitated after the intake of $Ag^+$ ions from Ag-NP by the bacterial cells which damages bacterial DNA and mitochondria, inactivates the bacterial enzymes and finally leads to cell death [41,44].

## 6. Conclusion

Resistance of pathogenic bacteria to antibiotics is a serious threat to public health. In this context Ag-NP has found a niche in our search for antimicrobial agents [45]. In conformity with the earlier observations on the toxic effect on bacteria we find that Ag-NP disrupts the cell morphology, causes DNA condensation and leads to the generation of ROS. The lag phase was found to increase in duration for the two bacteria with the increase in concentration of Ag-NP. The salient feature of this work is the modeling of the growth curves of *E. coli* and *S. aureus* after incorporation of a death term by using two commonly used mathematical models (Logistic and Gompertz). The Gompertz model is amenable to the treatment of death rate separately, which cannot be brought within the ambit of the Logistic model. This modification would be useful to model the effect of any bactericidal molecule. Additionally, mutations in many of the house-keeping genes and repair proteins can be lethal to an organism [46], and the effect of such a mutation on the growth can be associated with the induction of death, thus showing the wider ramification for the applicability of the modified model.

## Ackowledgments

TC has been supported by grants from the Department of Science and Technology (SR/WOS-A/LS-390/2011). Authors are grateful to Dr. Achintya Singha for his help with the synthesis of silver nanoparticles

and characterization. Authors also acknowledge Dr. Jaspreet S. Grewal for his help with fluorescence microscopy and Ms. Shamila Sarwar for scanning electron microscopy.

## Appendix A. Supplementary data

Additional results are given in five figures. Fig. S1 provides the absorption spectrum of Ag-NP. Fig. S2 describes the TEM data. Fig. S3 displays the colony counting assay of normal and Ag-NP treated *E. coli* and *S. aureus* cells. Flow cytometric analyses are shown in Fig. S4. The graphs representing the variation of OD and CFU/mL with time for *E. coli* and *S. aureus* are shown in Fig. S5. Supplementary data to this article can be found online at http://dx.doi.org/10.1016/j.bbagen.2014.10.022.

## References

[1] K. Kovarove-Kovar, T. Egli, Growth kinetics of suspended microbial cells: from single-substrate-controlled growth to mixed-substrate kinetics, Microbiol. Mol. Biol. Rev. 62 (1998) 646–666.
[2] P.K. Malakar, G.C. Barker, M.H. Zwietering, K. van't Riet, Relevance of microbial interactions to predictive microbiology, Int. J. Food Microbiol. 84 (2003) 263–272.
[3] K.K. Schultze, R.H. Linton, M.A. Cousin, J.B. Luchansky, M.L. Tamplin, A predictive model to describe the effects of temperature, sodium lactate, and sodium diacetate on the inactivation of a serotype 4b strain of *Listeria monocytogenes* in a frankfurter slurry, J. Food Prot. 69 (2006) 1552–1560.
[4] I. Mytilinaios, M. Salih, H.K. Schofield, R.J.W. Lambert, Growth curve prediction from optical density data, Int. J. Food Microbiol. 154 (2012) 169–176.
[5] S. Lopez, M. Prieto, J. Dijkstra, M.S. Dhanoa, Statistical evaluation of mathematical models for microbial growth, Int. J. Food Microbiol. 96 (2004) 289–300.
[6] J. Baranyi, T.A. Roberts, P.J. McClure, A non-autonomous differential equation to model bacterial growth, Food Microbiol. 10 (1993) 43–59.
[7] R.C. McKellar, A heterogeneous population model for the analysis of bacterial growth kinetics, Int. J. Food Microbiol. 36 (1997) 179–186.
[8] R. Pearl, The growth of populations, Q. Rev. Biol II (4) (1927) 532–548.
[9] M. Peleg, M.G. Corradini, Microbial growth curves: what the models tell us and what they cannot, Crit. Rev. Food Sci. Nutr. 51 (2011) 917–945.
[10] H. Fujikawa, A. Kai, S. Morozumi, A new logistic model for *Escherichia coli* growth at constant and dynamic temperatures, Food Microbiol. 21 (2004) 501–509.
[11] B. Gompertz, On the nature of the function expressive of the law of human mortality, and on a new mode of determining the value of life contingencies, Philos. Trans. R. Soc. Lond. 115 (1825) 513–585.
[12] A.M. Gibson, N. Bratchell, T.A. Roberts, Predicting microbial growth: growth responses of *Salmonella* in a laboratory medium as affected by pH, sodium chloride and storage temperature, Int. J. Food Microbiol. 6 (1987) 155–178.
[13] G.D. Wright, Resisting resistance: new chemical strategies for battling superbugs, Chem. Biol. 7 (2000) 127–132.
[14] G.D. Wright, Bacterial resistance to antibiotics: enzymatic degradation and modification, Adv. Drug Deliv. Rev. 57 (2005) 1451–1470.
[15] C.L. Gyles, Shiga toxin-producing *Escherichia coli*: an overview, J. Anim. Sci. 85 (2007) 45–62.
[16] O. Bahcall, MRSA toxicity and virulence, Nat. Genet. 46 (2014) 423.
[17] D.A. Groneberg, M. Giersig, T. Welte, U. Pison, Nanoparticle-based diagnosis and therapy, Curr. Drug Targets 7 (2006) (2006) 643–648.
[18] S. Nie, Y. Xing, G.J. Kim, J.W. Simons, Nanotechnology applications in cancer, Annu. Rev. Biomed. Eng. 9 (2007) 257–288.
[19] J.S. Kim, E. Kuk, K.N. Yu, J.H. Kim, S.J. Park, H.J. Lee, S.H. Kim, Y.K. Park, Y.H. Park, C.Y. Hwang, Y.K. Kim, Y.S. Lee, D.H. Jeong, M.H. Cho, Antimicrobial effects of silver nanoparticles, Nanomedicine 3 (2007) 95–101.
[20] J.R. Morones, J.L. Elechiguerra, A. Camacho, K. Holt, J.B. Kouri, J. Tapia, M.J. Yacaman, The bactericidal effect of silver nanoparticles, Nanotechnology 16 (2005) 2346–2353.
[21] R. Mahendra, Y. Alka, G. Aniket, Silver nanoparticles as a new generation of antimicrobials, Biotechnol. Adv. 27 (2009) 76–83.
[22] H.H. Lara, N.V. Ayala-Nuñez, L. Ixtepan-Turrent, C. Rodriguez-Padilla, Mode of antiviral action of silver nanoparticles against HIV-1, J. Nanobiotechnol. 8 (2010) 1.
[23] P.D. Bragg, D.J. Rainnie, The effect of silver ions on the respiratory chains of *Escherichia coli*, Can. J. Microbiol. 20 (1974) 883–889.
[24] W.R. Li, X.B. Xie, Q.S. Shi, H.Y. Zeng, Y.S. Ou-Yang, Y.B. Chen, Antibacterial activity and mechanism of silver nanoparticles on *Escherichia coli*, Appl. Microbiol. Biotechnol. 85 (2010) 1115–1122.
[25] S. Pal, Y.K. Tak, J.M. Song, Does the Antibacterial aactivity of silver nanoparticles depend on the shape of the nanoparticle? A study of the Gram-negative bacterium *Escherichia coli*, Appl. Environ. Microbiol. 73 (2007) 1712–1720.
[26] G.A. McFeters, F.P. Yu, B.H. Pyle, P.S. Stewart, Physiological assessment of bacteria using fluorochromes, J. Microbiol. Methods 21 (1995) 1–13.
[27] J. Porter, C. Edwards, R.W. Pickup, Rapid assessment of physiological status in *Escherichia coli* using fluorescent probes, J. Appl. Bacteriol. 79 (1995) 399–408.
[28] B.I. Tarnowski, F.G. Spinale, J.H. Nicholson, DAPI as a useful stain for nuclear quantitation, Biotech. Histochem. 66 (1991) 296–302.
[29] D.D. Ross, C.C. Joneckis, J.V. Ordonez, A.M. Sisk, R.K. Wu, A.W. Humburger, R.E. Nora, Estimation of cell survival by flow cytometric quantification of fluorescein diacetate/propidium iodide viable cell number, Cancer Res. 49 (1989) 3776–3782.
[30] D. Guo, L. Zhu, Z. Huang, H. Zhou, Y. Ge, W. Ma, J. Wu, X. Zhang, X. Zhou, Y. Zhang, Y. Zhao, N. Gu, Anti-leukemia activity of PVP-coated silver nanoparticles via generation of reactive oxygen species and release of silver ions, Biomaterials 34 (2013) 7884–7894.
[31] Q.L. Feng, J. Wu, G.Q. Chen, F.Z. Cui, T.M. Kim, J.O. Kim, A mechanistic study of the antibacterial effect of silver ions on *Escherichia coli* and *Staphylococcus aureus*, J. Biomed. Mater. Res. 52 (2000) 662–668.
[32] J.A. Creighton, C.G. Blatchford, M.J. Albrecht, Plasma resonance enhancement of Raman scattering by pyridine adsorbed on silver or gold sol particles of size comparable to the excitation wavelength, J. Chem. Soc. Faraday Trans. 75 (1979) 790–798.
[33] J. Monod, The growth of bacterial cultures, Annu. Rev. Microbiol. 3 (1949) 371–394.
[34] P. Irwin, J. Martin, L.H. Nguyen, Y. He, A. Gehring, C.Y. Chen, Antimicrobial activity of spherical silver nanoparticles prepared using a biocompatible macromolecular capping agent: evidence for induction of a greatly prolonged bacterial lag phase, J. Nanobiotechnol. 8 (2010) 34.
[35] J.A. Myers, B.S. Curtis, W.R. Curtis, Improving accuracy of cell and chromophore concentration measurements using optical density, BMC Biophys. 6 (2013) 4.
[36] U. Klueh, V. Wagner, S. Kelly, A. Johnson, J.D. Bryers, Efficacy of silver-coated fabric to prevent bacterial colonization and subsequent device-based biofilm formation, J. Biomed. Mater. Res. 53 (2000) 621–631.
[37] R. Kumar, S. Howdle, H. Munstedt, Polyamide/silver antimicrobials: effect of filler types on the silver ion release, J. Biomed. Mater. Res. 75 (2005) 311–319.
[38] I. Sondi, B. Salopek-Sondi, Silver nanoparticles as antimicrobial agent: a case study on *E. coli* as a model for Gram-negative bacteria, J. Colloid Interface Sci. 275 (2004) 177–182.
[39] M. Yamanaka, K. Hara, J. Kudo, Bactericidal actions of a silver ion solution on *Escherichia coli*, studied by energy-filtering transmission electron microscopy and proteomic analysis, Appl. Environ. Microbiol. 71 (2005) 7589–7593.
[40] B. Gibbins, L. Warner, The role of antimicrobial silver nanotechnology, Med. Device Diagn. Ind. Mag. 1 (2005) 1–2.
[41] M. Raffi, F. Hussain, T.M. Bhatti, J.I. Akhter, A. Hameed, M.M. Hasan, Antibacterial characterization of silver nanoparticles against *E. coli* ATCC-15224, J. Mater. Sci. Technol. 24 (2008) 192–196.
[42] J. Thopmas, S.D. Kahne, S. Walker, The bacterial cell envelope, Old Spring Harb. Perspect. Biol. 2 (2010) a000414.
[43] K. Soo-Hwan, H.S. Lee, D.S. Ryu, S.J. Choi, D.S. Lee, Antibacterial activity of silver nanoparticles against *Staphylococcus aureus* and *Escherichia coli* Korean, J. Microbiol. Biotechnol. 39 (2011) 77–85.
[44] R.G.E. Murray, P. Steed, H.E. Elson, The location of the mucopeptide in sections of the cell wall of *Escherichia coli* and other Gram-negative bacteria, Can. J. Microbiol. 11 (1965) 547–560.
[45] Q.H. Tran, V.Q. Nguyen, A.T. Le, Silver nanoparticles: synthesis, properties, toxicology, applications and perspectives, Adv. Nat. Sci.: Nanosci. Nanotechnol. 4 (2013) 033001.
[46] E. Kim, J.D. Lowenson, D.C. MacLaren, S. Clarke, S.G. Young, Deficiency of a protein-repair enzyme results in the accumulation of altered proteins, retardation of growth, and fatal seizures in mice, Proc. Natl. Acad. Sci. U. S. A. 94 (1997) 6132–6137.